Research paper

Calculating the maximum thrust generated per second by a model ionic engine when a cosmic ray source is incident on it using OpenMC

Sivani Satya Sai Sri Naga Vemparala

Abstract:
The ionic engine design experienced a massive surge in popularity from the early 1960's and its significance and achievements in the aerospace industry ever since have been nothing short of remarkable . The engine was first used on the SERT-1 in 1964 and later went on to be incorporated in various spacecrafts such as SMART-1, DeepSpace, Artemis,etc., all of which were important NASA missions. Additionally, they are being used as thrusters to maneuver over 100 Geostationary Earth-Orbit Communication satellites to ensure they stay in the desired orbit and operate for a longer period of time. A fundamental problem of the ionic engine is its inability to release large amounts of thrust, making it useful for only in-space propulsion and impractical for launching rockets which require large amounts of energy. This research paper explores the viability in modeling the internal compartments of the engine using various materials and assessing the benefits and challenges in using those materials for the engine. Doing so, the paper wishes to introduce an effective way of enabling conversion of cosmic radiation incident on the compartments into alpha particles and use them as a xenon ionizing source. In this manner, it can give a rough estimate of the total thrust the engine produces in a timeframe of one second. The task is accomplished by modeling the engine on OpenMC and running tallies on suitable parameters such as neutron flux, heating, absorption, etc. The primary aim of this research paper is to provide a general overview of the maximum thrust generated by the model ionic thruster located in deep space when a cosmic ray is incident on it using OpenMC, to obtain the calculation results, and circuit mapping.

Keywords : Cosmic radiation, materials, alpha particles, OpenMC, circuit mapping, thrust

Table of contents:

Introduction and Historical Context:

The ionic thruster is a special class of engines that accelerates ionized propellant (xenon or krypton) by means of an electric field to generate plasma. A hollow cathode acts as the electron source removing thermions from a charged metal surface once the metal's thermal vibrational energy has overcome the electrostatic forces holding its electrons to the surface, a process known as thermionic emission [1]. Ionic engines are operated using either electrostatic or electromagnetic fields. Current ionic thrusters such as the NSTAR (NASA Solar Electric Propulsion Technology Application Readiness) and NEXT (NASA's Evolutionary Xenon Thruster) can produce a thrust of up to 92mN and 236 mN respectively [2]. The gridded ion-thruster, theoretically advanced by German-American physicist Ernst Stuhlinger in the 1950's and designed by American physicist Harold Kaufman in the 1960's, is a thruster having a high specific impulse, high thrust efficiency and precise thrust control. Its three main components are: Ionization chamber, neutralizer and the accelerator grid. Incoming electrons from a hollow cathode collide with the atoms of a gas having a relatively higher atomic radius, such as xenon, and ionize it in the ionization chamber. The cations are then propelled to high

speeds using an accelerator grid consisting of the electric field and are subsequently slowed down using a decelerator grid which has a negative potential and is positioned downwards to prevent them from losing directionality. The neutralizer, or the hollow cathode, predominantly neutralizes the positive charge and helps in preventing buildup of excess positive charge, which is accelerated towards the rear end of the engine as mentioned earlier, on the spacecraft by releasing electrons which in turn helps create plasma. Strong magnets are installed on either side of the ionization chamber to confine the plasma generated [3]. Cosmic radiation is a highly ionizing type of radiation originating from supernovae explosions, solar flares, other energetic events, etc. in space and is accelerated by astrophysical sources. Primary cosmic rays are the naturally occurring subset of the GCR's (Galactic cosmic rays) consisting of nucleons of almost all elements on the periodic table. 80% of these nucleons are protons, 15% are helium nuclei (alpha particles), 2% are electrons, 1% are heavier nuclei and 0.2% are lighter nuclei of elements (other than H and He) on the periodic table. The nuclei of heavy and light elements involved in the cosmic rays are stable in nature. The energy of the high-speed protons prevailing abundantly in cosmic rays ranges from 100 MeV to 10 GeV and has a speed ranging from 42.8% - 99.6% the speed of light [4].

Ionic engine model and compartments:

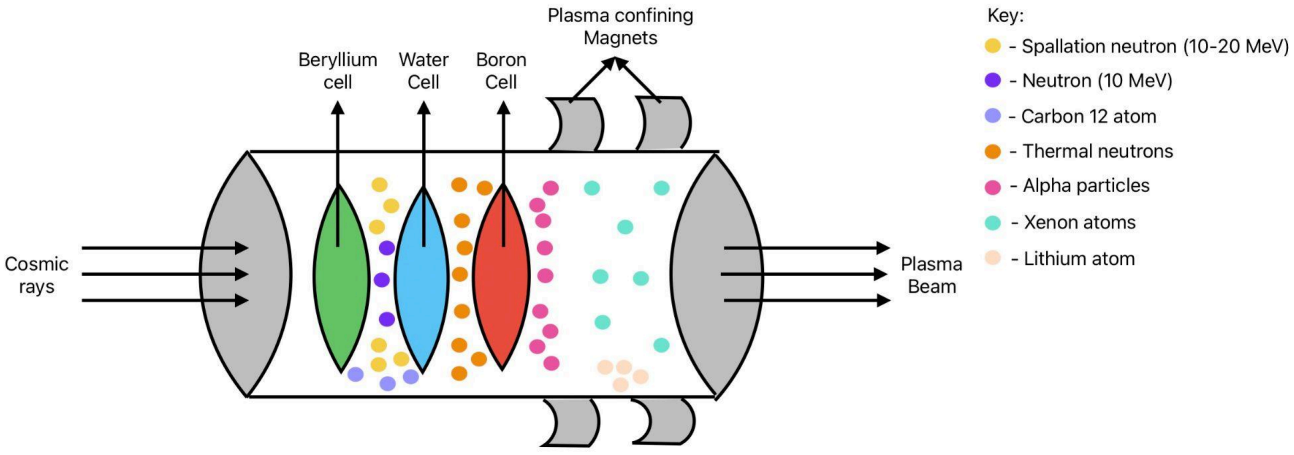

Figure 2: Scale model of ionic engine, Source: freeform

Region 1:

a. **Spallation and alpha particle bombardment:** Spallation is a type of nuclear reaction wherein energetic particles (such as high energy protons) interact with the nucleus of an atom onsetting a cascade process (or a violent chain reaction) where the typical production of spallation neutrons is 2 but may vary by circumstance [5] . It occurs when

the energy of the incident particle exceeds 100 MeV. By using beryllium as the spallation target, one can minimize the post-collision neutron interactions otherwise encountered on using other material targets and absorb a larger number of neutrons. In addition to this, its low atomic mass and high neutron yield per incident particle make it a suitable choice for the first internal compartment. High – energy protons when bombarded on beryllium atoms (the target) react violently with the latter and disintegrate it into a neutron and several other constituents (such as alpha particles, protons, etc.) through spallation. Although spallation is commonly observed for elements with high -Z (lead, tungsten, etc.) it is equally possible in low – Z targets (lithium, beryllium, etc.). Spallation with beryllium produces a neutron and boron-9 atom [6].

$p+{}_4Be^9 \rightarrow {}_5B^9+n$ ------ (1)

The ${}_5B^9$ undergoes beta positive decay to produce an electron neutrino and a positron and thus, emits bremsstrahlung radiation. It is defined as the braking radiation given off by free electrons which are deflected by the nuclei of atoms and electric fields of the charged particles within the atom [7]. Apart from spallation, the alpha particles in the cosmic rays collide with the beryllium particles to release neutrons and a stable C-12 atom, a process known as alpha particle bombardment on a beryllium foil, triggering further neutron production [8].

${}_4Be^9 + {}_2He^4 \dashrightarrow {}_6C^{12} + {}_0n^1$ ------- (2)

b. **Moderator*:*** The second junction will consist of a moderator which is a material that effectively converts high speed neutrons into slow thermal neutrons and makes them suitable for thermal neutron capture. Materials such as concrete, graphite or water, beryllium are commonly used as moderators. Having established the fact that both beta radiation and fast neutrons are being emitted in the processes occurring in region 1, water would be an excellent choice to fulfill the model's dual needs considering its ability to block beta radiation effectively [9].

c. **Thermal neutron capture*:*** The thermal neutrons produced are then passed through a boron foil. Boron is an excellent neutron absorber and can help control the rate at which the reaction occurs, similar to its function as a control rod in nuclear reactors. Boron does not produce any radiation of its own except for a stable isotope of lithium and an alpha particle [10].

${}_5B^{10}+10n \rightarrow {}_3Li^7+ {}_2He^4(\alpha)$. -----(3)

Region 2: The alpha particles produced collide with injected xenon atoms and thus undergo ionization. Having the strongest ionizing power among beta, gamma and x-rays, they are most effective at stripping electrons from elements after collision with them. Additionally, they travel at a top speed of about 5-7% the speed of light and are heavier and slower in nature [11], making it feasible to stop them by a few layers of almost any material. They knock out Xe+ and electrons

from the xenon atom and subsequently collide with either another xenon atom or with the walls of the region before losing energy. The anode present in the ionization chamber accelerates the protons towards the aft end of the ionic thruster where millions of tiny coaxial apertures focus the incident rays and produce a parallel beam from it. The protons then pass through a screen grid, which contains a positively charged electrode, and then through an accelerator grid, which contains a negatively charged electrode, where they are accelerated to high speeds due to the strong electric field generated between the two electrodes. Electrons, as per their alternate function in ionic engines, neutralize the beam of positive charge accumulating outside the spacecraft.

Additional chambers:

Overhead region 1, an additional anode is present which redirects the incident 2% cosmic ray electrons towards the neutralizer present closely outside the second region. The circuit connections for the additional anode will be mentioned in the circuit mapping section of this paper.

Material composition:

a. **Region 1:**

The region enclosure is made of tungsten which offers the benefit of having an extremely high melting point, stability and hardness. The C-12 atom produced during alpha particle bombardment settles down (as it is comparatively heavier) and reacts with the tungsten walls at high temperatures to form tungsten carbide ($CW4$). This helps in strengthening the layer by increasing its impact resistance, compressive strength, resistance to deformation, deflection, oxidation and its melting point to 2785 degrees celsius. [12].

b. Region 2 :

Again, the region requires thick layers of tungsten to mitigate the effect of extremely high temperatures on its inner walls as a result of plasma formation. Moreover, the low penetrating power of alpha particles means that their motion can be stopped by even a few layers of tungsten.

Circuit mapping:

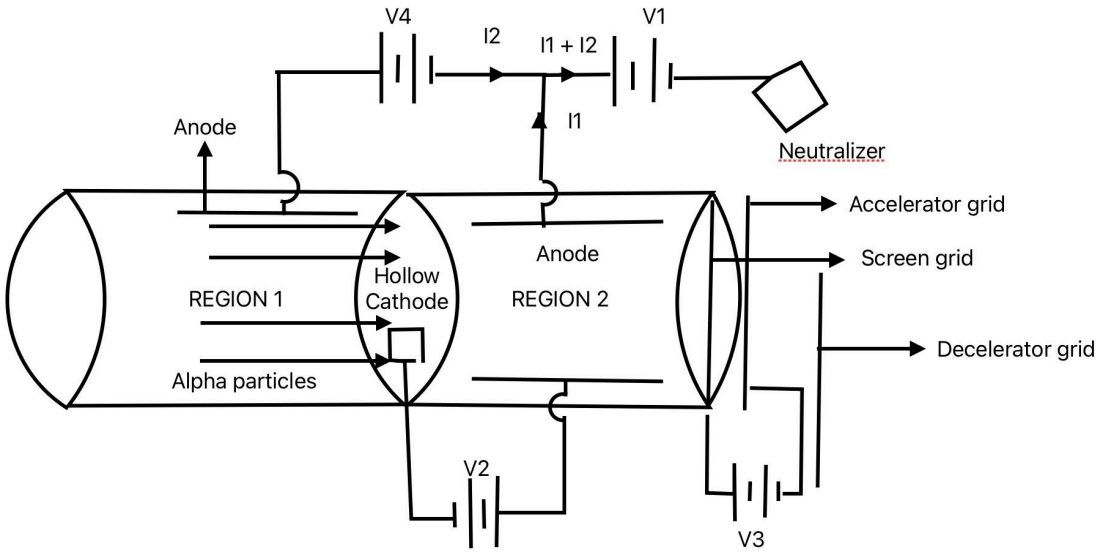

Figure 3: Circuit diagram of ionic engine model, Source: Freeform

The circuit mapping possesses a striking resemblance to that of the gridded ion thruster but differs only by a circuit that redirects the incoming electron constituency towards the neutralizer at the rear end of the engine [13]. Here, V1, V2, V3 and V4 symbolize the three voltage sources in the circuit. I1 and I2 are used to describe the flow of current within the circuit due to the presence of moving electrons. Using Kirchoff's current law, which states that the algebraic sum of the currents entering a junction at a nodal point is equal to the sum of the currents leaving, a total of I1 + I2 current now flows in the branch of the circuit connected to the neutralizer and helps balance the excess positive charge buildup. Thus, the electrons flowing to the neutralizer hail from two sources: the anode present on the upper wall of region 1 and the anode present on the upper wall of region 2. The electrons produced on alpha particle collision with xenon atoms contribute to the process of ionization by being reemitted via the hollow cathode after passing through the anode present on the lower wall of region 2. The electrons further contribute to the electric field generated between the screen grid and the accelerator grid.

Assumptions and tallies:

The source for this model entails a cosmic ray source which is isotropic in nature and for purposes of convenience is emitted from a point source located in deep space. The model assumes 100% efficiency. Reaction between lithium and tungsten has not been considered as the product is usually formed in presence of oxygen. The operational power of the ionic thruster has been taken as 12kW, although experimental models proved to be capable of achieving a total of 35kW [14]. The high power consumption allows the engine to produce large amounts of thrust and be accommodative of even higher ranges. The CSG model of the engine is a tungsten cylinder of radius 90 cm and length 100 cm enclosing a hexagonal lattice consisting of

18 spherical water cells and 18 spherical boron cells each of radius 10 cm respectively. Although 1-2 cm of water is sufficient to shield against bremsstrahlung radiation, [16] 10 cm has been assumed to allow admission of a greater number of neutrons. Furthermore, the radius of the boron foil layer has also been taken as 10 cm to maintain uniformity and ensure simplified calculations. The collisions of heavier and lighter nuclei with the thruster are negligible. 10,000 cosmic ray particles each having an energy of 10 MeV are incident in batches of 10 on the ionic thruster. A rough estimate of the time interval between the collision of 2 batches of 10,000 cosmic ray particles on the thruster has been calculated keeping in mind a higher incident energy source means a lower chance of frequent collision with the thruster. This estimate yields the result of 10,000 particles each having an energy of 10 MeV hitting the thruster per square meter with an average relaxation time of 0.01 seconds [15]. Since 80% of the cosmic ray particles are high-energy protons (that means 8000 protons), the total number of spallation neutrons produced on collision with the beryllium foil (for convenience, 8000 beryllium atoms) will be 16000. These calculations compensate for OpenMC's inability to perform and tally the results of spallation. Furthermore, OpenMC cannot produce tallies for neutron energies greater than 20 MeV and so the neutrons emitted after spallation will assume an energy value within the range of 10- 20 MeV. For purposes of thrust calculation, the spallation neutron energy will be set to a singular value of 20 MeV. The secondary derivatives of this reaction are 8000 unstable ${}_5B^9$ radioactive isotopes which emit 8000 stable isotopes of ${}_4Be^9$ and bremsstrahlung radiation. Spallation depends on material thickness; a thinner foil of beryllium will increase the stress on the material and will be highly unreliable and unsafe. The beryllium foil, thus, will have an optimum thickness of 7.6mm. 15% of the cosmic ray particles consist of alpha particles (1500 alpha particles); as per equation 2, the total number of neutrons and carbon – 12 atoms thus produced will be 1500. The energy of the emitted neutron will be 10 MeV. The incident neutron energy can henceforth be divided into two classes: 16000 neutrons having an energy of 20 MeV and 1500 neutrons having an energy of 10 MeV.

OpenMC Modelling and Simulations :

The hexagonal lattice model has been narrowed down in terms of appearance and function to meet the requirements of the ionic engine design. The lattice is composed of an equal number of water and boron cells, each acting as a medium of conversion. The innermost cell of the lattice can either be water or boron, however, this differentiating factor yields different neutron flux results.

With boron as the inner cell of the universe (Case 1)	**With water as the inner cell of the universe (Case 2)**

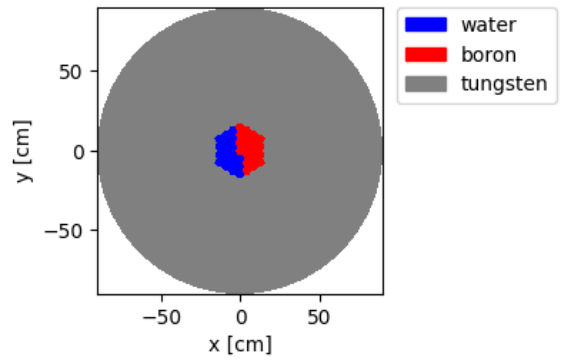

Figure 4: Cross-sectional view of CSG model from the xy plane, Source : OpenMC

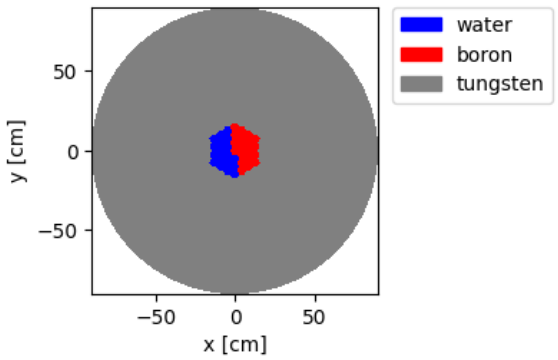

Figure 4: Cross-sectional view of CSG model from the xy plane, Source : OpenMC

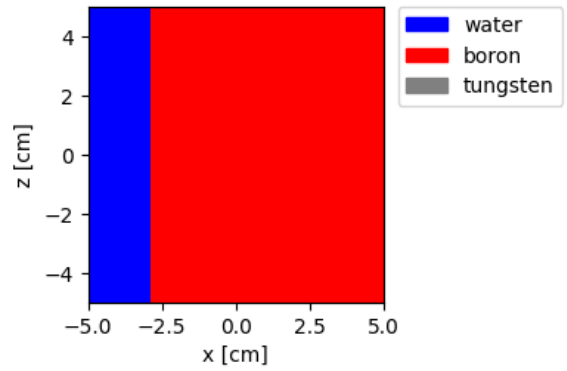

Figure 5: Cross-sectional view of CSG model from the xz plane, Source : OpenMC

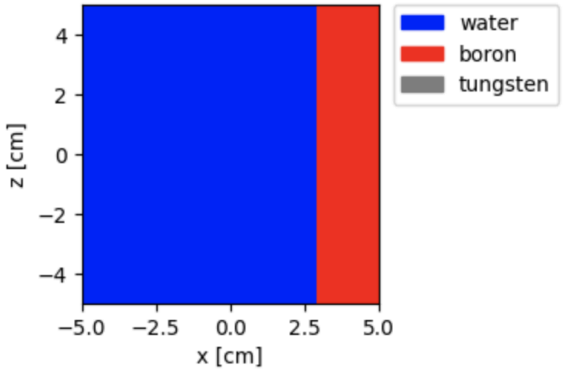

Figure 7: Cross-sectional view of CSG model from the yz plane, Source : OpenMC

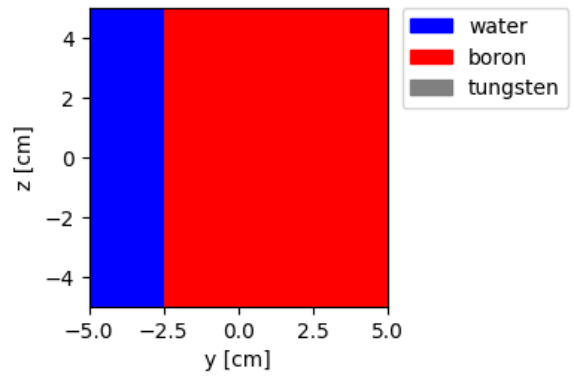

Figure 6: Cross-sectional view of CSG model from the yz plane, Source : OpenMC

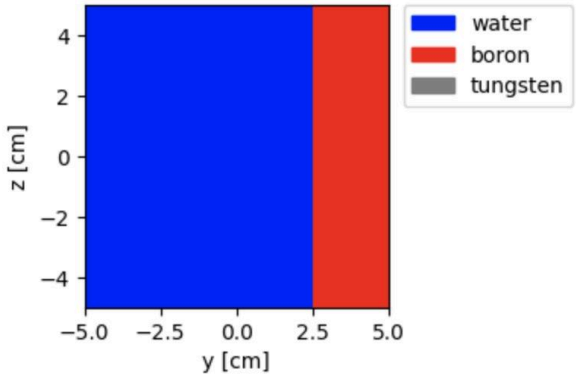

Figure 8: Cross-sectional view of CSG model from the yz plane, Source : OpenMC

Figure 4 visually represents the assumed model as seen from the xy-plane. Figure 5 and Figure 6 portray the view of the model as seen from the xz and yz-plane. The model's innermost cell consists of boron and yields a maximum neutron flux of 2.40301701e+11 neutrons per cm2 per second. On the other hand, Figure 7 and 8 represent the xz and yz-plane of the model with its innermost cell as water. This model generates a maximum neutron flux of 3.38547002e+11 neutrons per cm2 per second. A higher neutron flux will guarantee a larger number of alpha particles being produced by boron leading to a subsequent increase in thrust generated. Hence, the second case of the model will be considered for further calculations.

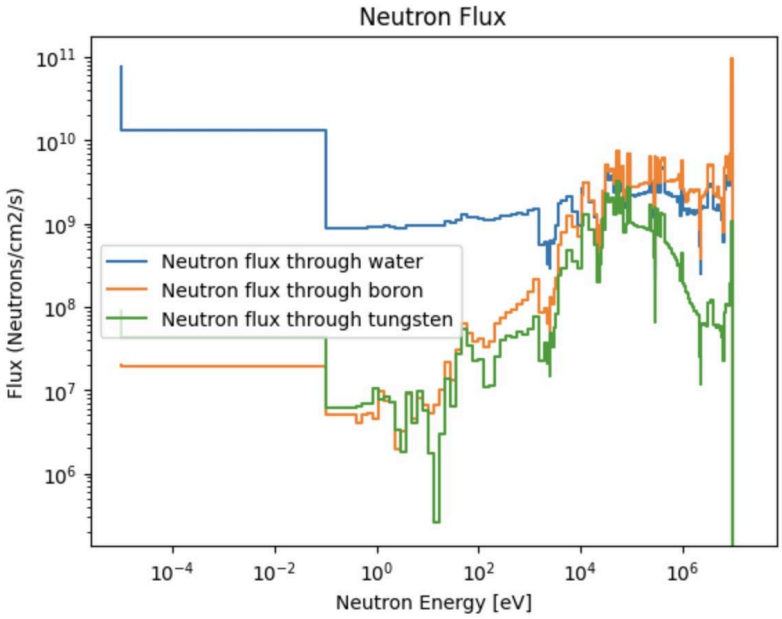

(Figure 9: Neutron flux in neutrons per cm^2 per second for 17500 incident neutrons, Source : OpenMC)

The units of neutron flux on OpenMC are neutrons emitted per source neutron. To obtain the neutron flux in units of neutrons per cm^2 per second, the flux value calculated on OpenMC must be multiplied by the neutron source rate and divided by the volume. The neutron source rate for the model has been calculated by dividing power by energy (converted into joules). The value is then divided by the corresponding volume: volume of tungsten cylinder and volume of spherical water and boron pincells located within the lattice respectively.

$$Neutron\ flux\ = \frac{OpenMC\ flux \times Neutron\ source\ rate}{Volume}$$

The initial neutron flux is highest for water, intermediate for tungsten and lowest for boron. The concomitant values experience a sudden drop in admission of neutrons at about 0.50 eV with the fall in neutron flux for water being relatively lower as opposed to tungsten and boron. The rate of change in neutron flux for water does not fluctuate as vigorously as that of tungsten and boron, which fall to their lowest values at around 30-50 eV before gradually rising and again declining after which, like water, they extend to infinity. In a sense, the increased neutron flux through water and boron has its advantages and disadvantages; it increases the number of xenon atoms being ionized but such an increase must be compensated by adequate material strength of shielding component to counteract the damaging changes its interaction with the material can bring. However, the neutron flux through tungsten is also increasing rapidly and excessive neutron irradiation on the material leads to its decay and transmutation into rhenium and osmium isotopes leading to its embrittlement.

Neutron flux distribution as a function of spallation neutron energy: (10 MeV, 12 MeV, 15 MeV, 17 MeV respectively)

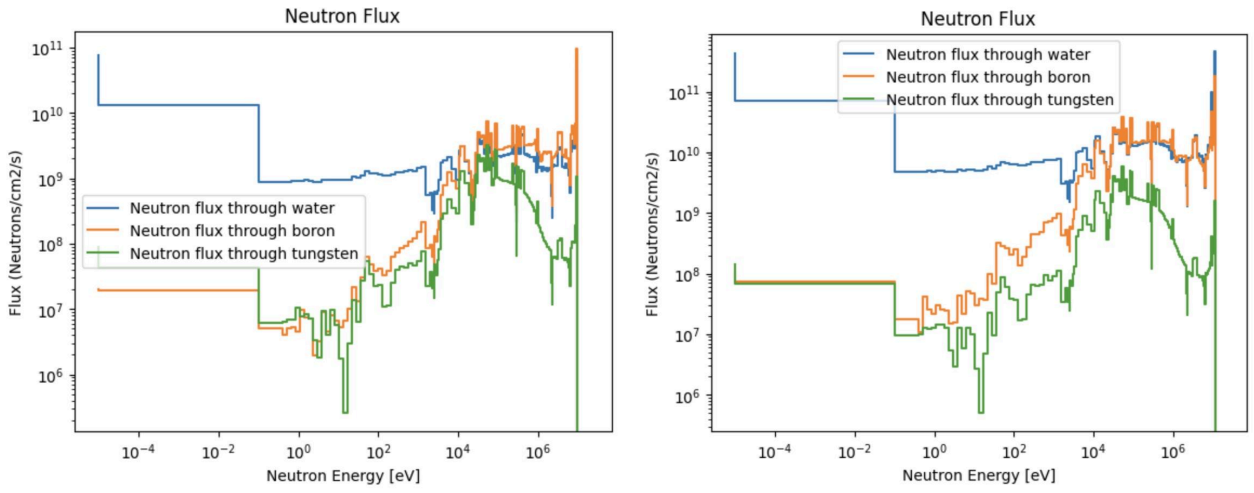

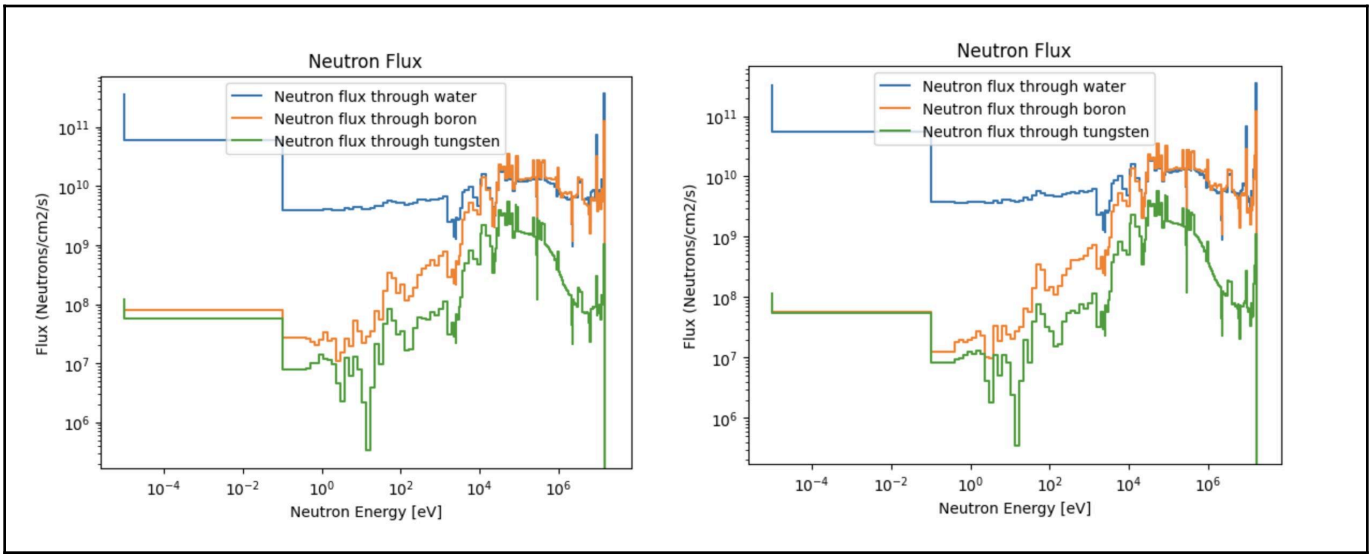

The graphs give a brief idea of the neutron flux produced for certain values corresponding to the set range. A difference in the initial neutron flux for boron and tungsten at lower neutron energies (range of 0-10 $^{-1}$eV) can be observed at 10 MeV but the difference becomes less discernible when the incident neutron energy is 17 MeV. The gap between neutron flux production of boron and tungsten for the energy value of 10 $^{-4}$ eV widens as the incident neutron energy increases from 10 eV to 12 eV and becomes constant thereafter, only slightly decreasing when the incident neutron energy is 17 eV. The graphs exhibit an overall consistency in terms of neutron flux production for varying incident neutron energy values.

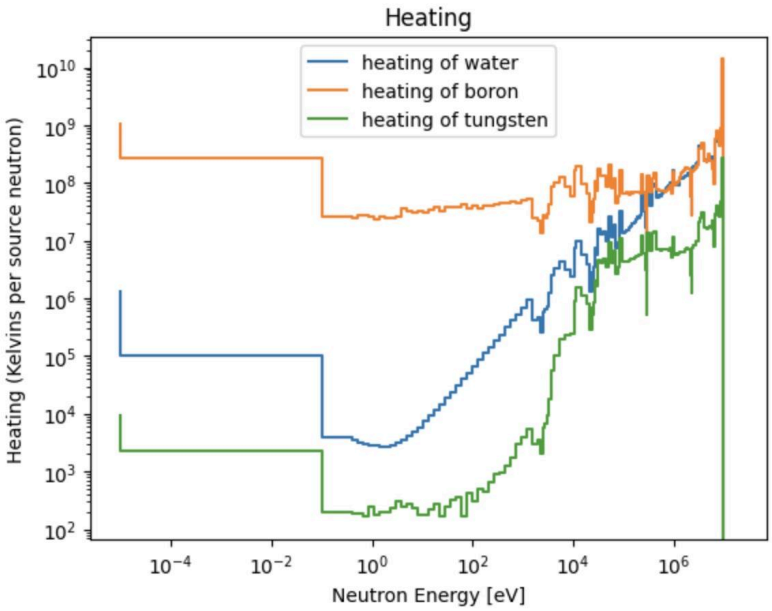

(Figure 10: Heating of tungsten, boron and water when 17500 neutrons are incident on the engine, Source : OpenMC)

The units of heating on OpenMC are eV. We need to convert this into kelvins.

$$Joules = eV \times 1.602 \times 10^{-19}$$

This converts eV into joules.

$$Kelvins = \frac{Joules}{1.380 \times 10^{-23}}$$

In this way, the value of heating in kelvins has been calculated and graphed. The graphs produced are almost congruent to the ones observed previously with the primary difference solely being the order in which the materials get heated the most. Tungsten has the highest heat resistance among all having an initial rise in temperature of about 5000-10000 kelvins at an incident neutron energy of approximately 0.00001 eV, followed by water and boron which get heated to a temperature of around $10^5 - 10^6$ kelvins and 10^9 kelvins respectively for the same incident energy. Water's heat resistance falls off as the incident neutron energy reaches 10 MeV but tungsten's resistance remains comparatively higher. An energy source of 20 MeV would certainly cause substantial amounts of heating, increasing the heat generated to >10^{10} kelvins per source neutron as depicted by the graph. This possesses strong disadvantages in

the context of neutron irradiation as it makes the model suitable for only a few batches (in this case 10) of cosmic radiation and not more.

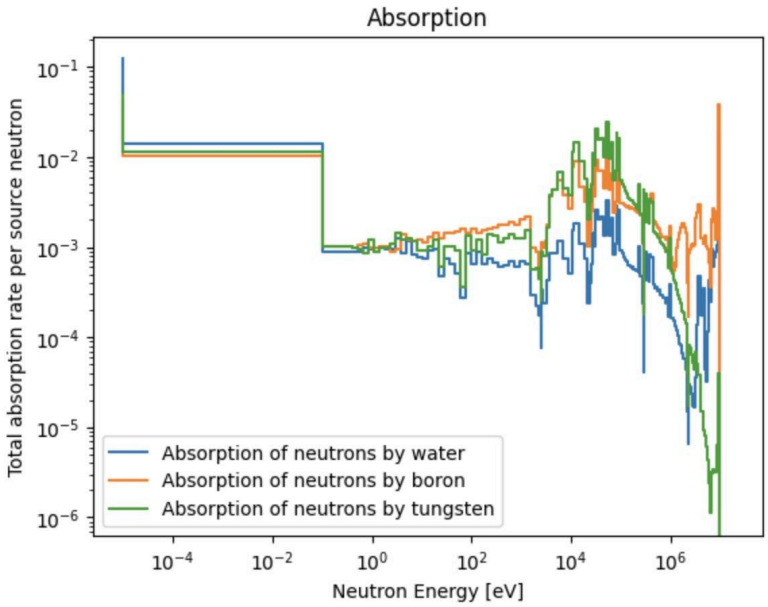

(Figure 11: Absorption rate of incident neutrons per source neutron for water, boron and tungsten, Source : OpenMC)

A similar absorption rate can be observed in all the materials. Water begins to absorb a higher amount of neutrons incident on it as compared to tungsten and boron by a narrow margin. The rate of absorption increases similarly for all materials after which it reduces gradually before rising infinitely. The neutron absorption becomes scattered with increasing energy as all the materials absorb all the neutron energy incident on it, with the rate being highest for boron.

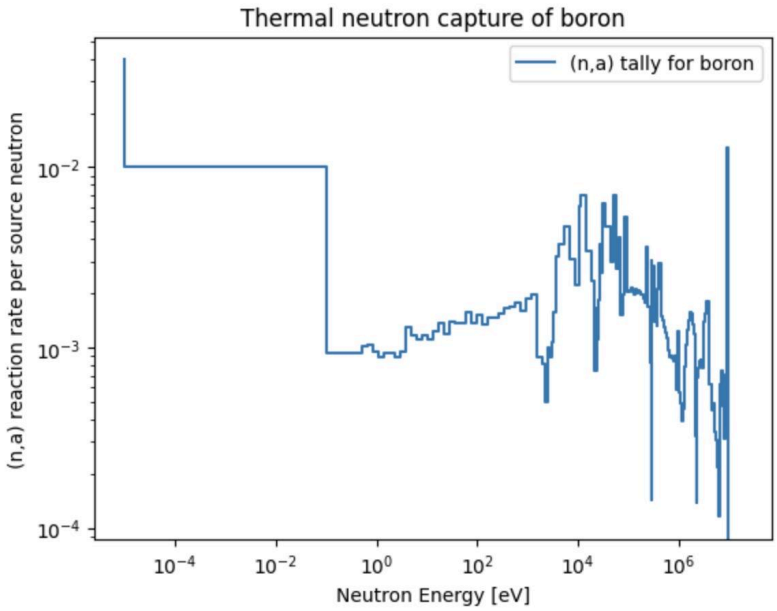

(Figure 12: (n,alpha) reaction rate when neutrons are incident on boron, Source : OpenMC)

The graph underscores the extremely fast reaction rate of the incident neutrons with the boron foil, followed by a drastic reduction and then a gradual increase in the number of reactions taking place as the energy of the incident neutron increases. The number of reactions taking place thereafter decreases before increasing infinitely. The purpose of this observation is to demonstrate the rate at which energy generation takes place.

Calculations:

I. **Bremsstrahlung radiation intensity:**

It is directly proportional to the square of the atomic number of the target (Z), the unit charge on the bombarding particle (z) and inversely proportional to the mass of the bombarding particle (m) [17]. Thus, intensity of the bremsstrahlung radiation reduces if the attacking particle is light. The atomic number of our spallation target (beryllium) is 4, the bombarding particle's (proton) unit charge is +1 and its mass is 1.67262192 × 10-27 kilograms. Using the relation, we have:

$$Radiation\ intensity = \frac{Z^2 z}{m}$$

$$= \frac{16 \times 1}{1.6726 \times 10^{-27}}$$

$$= 9.565 \times 10^{27}$$

This shows that the intensity of the bremsstrahlung radiation produced is very high for a proton producing a spallation neutron after collision with a beryllium atom. Fortunately, high levels of beta radiation can be effectively stopped by using a few centimeters of water.

II. **Thrust:**

The maximum number of neutrons being produced per cm2 per 0.01 seconds through boron as per OpenMC calculations is 3.38547002e+11 which means that these are also the maximum number of alpha particles being produced per source neutron collision with boron. Since the calculated average relaxation time is 0.01 seconds, we must multiply it by 100 to get the total number of neutrons being produced in a second which is 3.38547002e+13. The neutrons produced (20MeV and 10MeV) are in a ratio of 16:3 (the same ratio as the proton and alpha particle composition in cosmic rays). This means that 2.85e13 alpha particles have an energy of 20 MeV and the remaining 5.34e12 particles have an energy of 10 MeV. The ionization potential of xenon is around 12-13 eV; an indicator of the energy required to remove a valence electron from its isolated gaseous system. Dividing both 20 MeV and 10 MeV by 12eV (assuming) gives us the number of xenon atoms ionized by one alpha particle from both these energy sources respectively. Doing so, we obtain 1.66e6 atoms for the 20 MeV energy source and 8.33e5 atoms for the 10 MeV energy source. Using the unitary method, we now must calculate the total number of xenon atoms ionized by the alpha particles which collide with the atoms in the same ratio as mentioned earlier. Since the values for both these parameters have been obtained, we simply multiply them. As a result, a total of atoms for the 20 MeV energy is 4.731e19 source and 4.458e18 atoms for the 10 MeV energy source are being ionized. This gives us an estimated total of 5.1768e19 atoms being ionized within a time span of 1 second. Converting this value into grams gives us the change in mass of xenon per second.

$$N_a = n \times N_0 \times atomicity$$

$$n = \frac{W}{M}$$

$$5.1768 \times 10^{19} = \frac{W}{131.293} \times 6.022 \times 10^{23} \times 1$$

$$6.796 \times 10^{21} = W \times 6.022 \times 10^{23}$$

$$W = 0.001128\ grams$$

Where:

N_a = Number of xenon atoms

n = Number of xenon moles

N_0 = Avogadro's number

W = Mass of xenon
M = Atomic mass of xenon

A total of 0.001128 grams of xenon is being ionized by the thruster per second. This translates to 1.128e-6 kilograms of xenon being ionized per second. This is our propellant mass flow rate ($\frac{\Delta m}{\Delta t}$). To calculate the effective exhaust velocity, we must derive it from the kinetic energy equation.

$$E_k = \frac{1}{2}mv^2$$

$$v = \sqrt{\frac{2E_k}{m}}$$

Since the kinetic energy here is being produced in the form of electrical energy, we have;

$$v = \sqrt{\frac{2qV}{m}}$$

Where:
E_k = Kinetic energy
m = mass of xenon atom (in kilograms)
v = exhaust velocity
q = Charge of elementary particle
V = Operating voltage of thruster

Thus, the approximate exhaust velocity for a thruster with an operating voltage of 1000 volts is:

$$v \approx 38300\, m/s$$

$$Thrust = v\frac{\Delta m}{\Delta t}$$
$$= 38300\, m/s \times 1.128\ x\, 10^{-6}\, kg/s$$
$$= 0.0432\, N$$

This gives us the maximum thrust produced by the ionic engine model per second. This value is not reflective of the total thrust the thruster is capable of producing as the amount generated varies with the time duration of incidence. To get a rough idea of this, we must tabulate it.

Time interval between 17500 incident neutrons (in seconds)	Thrust (N)
10	0.432
100	4.32
1000	43.2
10000	432

This means by the end of 1000 seconds itself, there is enough thrust for the engine to continue its exploration into deep space. This value may recede if the number of incident neutrons reduces at a point of time.

Conclusions:

The ideal thrust generated by the low-energy incident neutrons approximates 0.0097282 newtons, a value that still hides the true potential of the effective thrust that can be generated. Typical thrusters possess thrusts of about 25-250 mN with a propulsive efficiency of about 65-80%. The results of this paper do not limit itself to a singular value considering cosmic rays, especially of low-energies, are present in abundance in space and are constantly incident on the thruster.

Limitations and Future work:

The model does not discuss the effects of heavy and light nuclei collision with the beryllium foil and subsequent layers of the thruster as this leads to the production of a number of radioactive isotopes which is a predicament that cannot be resolved by simple means and demands the construction of an engine capable of achieving structural integrity. This cannot be accomplished with modern standards due to the lack of appropriate centers that facilitate the testing of materials' performance under extreme physical conditions and a suitable environment, such as stress or heat [18]. Spallation neutrons typically exceed energies of 400-500 MeV [19] but OpenMC energy limitations means that the model's neutron energy production falls short of its actual scope. Water, boron and tungsten's ability to withstand heat gradually reduces as the incident neutron energy increases making it an impracticable process after 10 batches of neutron collisions as per the data obtained from the graph. Furthermore, high energy proton irradiation on tungsten (producing similar results to neutron irradiation) leads to the production of rhenium, tungsten and tantalum isotopes along with the emission of hydrogen and helium particles [20] which proves disastrous for the model and requires the usage of a material that can not only remain functional at high heat but also largely unreactive with the produced isotopes. One positive to note in this situation is that the half life of the most abundant

radioactive isotope of rhenium is 5×10^{10} years, suggesting its highly weak radioactivity and thus, slow decay [21]. Considering the closest material we have to meeting the model's demands and currently use to build shielding components of the engine is tungsten or a tungsten-rhenium alloy, future research must include the search for new materials (or its creation) that can consistently tolerate large amounts of heat without necessarily pushing up the space occupied and cope with the additional radioactive byproducts produced on increased incident energy cosmic ray collision with it. In addition, the creation of testing centers that allow simulation of the effects of heavy and light nuclei collision with the ionic thruster's internal and external compartments must be ensured. A practical approach towards tracking the thruster efficiency would be to simulate deep-space conditions within a suitable center along with the incidence of cosmic ray-like particles on the ionic thruster using separate instruments that emit its constituents, either separately or simultaneously, in the same ratio as the ray itself. This can give feedback on the performance of the model in a more gradual and effective manner as the quality of the material can be evaluated at each step, from the incidence of only one subset of the ray on the thruster (like protons) until the incidence of the entire ray.

Citations:

[1] Huffman, Fred. (2003). Thermionic Energy Conversion (Encyclopedia of Physical Science and Technology). Academic Press. https://doi.org/10.1016/B0-12-227410-5/00772-9
[2] NASA Glenn Research Centre. (2023, January 25). Gridded Ion Thrusters (NEXT-C). https://www1.grc.nasa.gov/space/sep/gridded-ion-thrusters-next-c/
[3] The Space Techie. (2021, February 10). Ionic Thruster: How it works?. https://www.thespacetechie.com/ion-thrusters-how-it-works/
[4] L'Annunziata, Micheal F. (2007). 6 - Cosmic Radiation. Elsevier Science B.V. https://www.thespacetechie.com/ion-thrusters-how-it-works/
[5] Jaegwon Yoo. (1998) .Neutron Production from Spallation Reactions. Proceedings of the Korean Nuclear Society Autumn Meeting. https://www.kns.org/files/pre_paper/30/98A-026.PDF
[6] Ahmed, Syed Naeem. (2015). 1- Properties and Sources of Radiation. Physics and Engineering of Radiation Detection (Second Edition). https://doi.org/10.1016/B978-0-12-801363-2.00001-2
[7] Stacy J, Vestrand W. (2003). Gamma-ray Astronomy. Encyclopaedia of Physical Science and Technology (Third Edition). https://doi.org/10.1016/B0-12-227410-5/00274-X
[8] Steven S. Zumdahl, Donald J. DeCoste. (2024). Chapter 19.Introductory Chemistry. https://www.vaia.com/en-us/textbooks/chemistry/introductory-chemistry-9-edition/chapter-19/problem-100-write-a-nuclear-equation-showing-the-bombardment/

[9] Ghosh, Sandip. (2024). 8.08 - Material selection and processing in nuclear safety. Comprehensive Materials Processing (Second Edition). https://doi.org/10.1016/B978-0-323-96020-5.00167-9
[10] Jin WH, Seldon C, Butkus M, Sauerwein W, Giap HB. A Review of Boron Neutron Capture Therapy: Its History and Current Challenges. Int J Part Ther. 2022 Jun 9;9(1):71-82. doi: 10.14338/IJPT-22-00002.1
[11] ARPANSA (Australian Radiation Protection and Nuclear Safety Agency). Alpha Particles. AustralianGovernment.https://www.arpansa.gov.au/understanding-radiation/what-is-radiation/ionising-radiation/alpha-particles#top
[12]Imetra. (2023). Tungsten Carbide Metal Properties. https://www.imetra.com/tungsten-carbide-material-properties/#:~:text=Hard%20and%20rigid%20yet%20has,oxidation%20with%20low%20temperature%20resistance.
[13] Yavuz, Burak & Turkoz, Emre & Celik, Murat. (2013). Prototype design and manufacturing method of an 8 cm diameter RF ion thruster. RAST 2013 - Proceedings of 6th International Conference on Recent Advances in Space Technologies. 619-624. 10.1109/RAST.2013.6581285.
[14] Lovtsov A, Selivanov M, Kostin A. (2020). Qualification status of high power ion thruster and flow control unit. Acto Astronautica. https://doi.org/10.1016/j.actaastro.2019.12.009
[15] CERN. (2024). Cosmic rays : particles from outer space. https://home.cern/science/physics/cosmic-rays-particles-outer-space
[16] IAEA (International Atomic Energy Agency). (2024). Radiation in everyday life. https://www.iaea.org/Publications/Factsheets/English/radlife#:~:text=Beta%20radiation%20consists%20of%20electrons,1%2D2%20centimetres%20of%20water.
[17] Yeung J, Campos A, Chan B, et al. Bremsstrahlung radiation. Reference article, Radiopaedia.org (Accessed on 10 Aug 2024) https://doi.org/10.53347/rID-14248
[18] GAO, U.S Government Accountability Office. (2023, March 30). Fusion Energy: Potentially Transformative Technology Still Faces Fundamental Challenges. https://www.gao.gov/products/gao-23-105813#:~:text=One%20key%20engineering%20challenge%20is,materials%20can%20be%20fully%20tested.
[19] Alpen, Edward L. (1998). Energy Transfer Processes. Academic Press, San Diego. https://doi.org/10.1016/B978-012053085-4/50007-7
[20] Rayaprolu R, Möller, S, Linsmeier, Ch, Spellerberg, S. 2016. Simulation of neutron irradiation damage in tungsten using higher energy protons. Nuclear Materials and Energy. https://doi.org/10.1016/j.nme.2016.09.008
[21] Abram U. 2003. 5.3- Rhenium. Comprehensive coordination chemistry II. https://doi.org/10.1016/B0-08-043748-6/04177-3